Separation control by tangential blowing inside the bubble

P. R. Viswanath, G. Ramesh, K. T. Madhavan

Abstract Experiments have been carried out investigating the effectiveness of steady tangential blowing (inside the separation bubble) to control an axisymmetric separated flow at low speeds. Turbulent boundary separation was induced on a contoured afterbody and the separated shear layer reattached on a narrow cylindrical sting. Measurements made consisted of model surface pressures, mean velocity, turbulent shear stress and kinetic energy profiles using a 2-component LDV system. The results explicitly demonstrate that blowing downstream of the separation location, but within the bubble, can be an effective means of separation control, considering both wall and wake flow reversals.

List of symbols

C_p	Static pressure coefficient ($= p - p_\infty/q_\infty$)
C_μ	Blowing momentum coefficient (2D)
$C_{\mu A}$	Blowing momentum coefficient (axisymmetric)
D	Model forebody diameter
h	Blowing slot height
k	$\langle u'^2 + v'^2 \rangle / 2$, Turbulent kinetic energy
m_{bl}	Boundary layer mass flow rate
m_j	Jet mass flow rate
p	Local surface pressure
p_∞	Freestream static pressure
q_∞	Freestream dynamic pressure
u	Local velocity in the boundary layer
U_∞	Freestream velocity
U_j	Jet velocity
$\langle u'^2 \rangle$	Mean square velocity fluctuation in x direction
$\langle v'^2 \rangle$	Mean square velocity fluctuation in y direction
τ	$\langle -u'v' \rangle$, Reynolds shear stress
δ^*	Boundary layer displacement thickness
θ	Boundary layer momentum thickness
x	Coordinate parallel to model axis
y	Coordinate normal to model axis

P. R. Viswanath, G. Ramesh, K. T. Madhavan
Experimental Aerodynamics Division
National Aerospace Laboratories, Bangalore 560 017, India

1
Introduction

The problem of turbulent boundary layer separation and the associated aerodynamic effects have been the subject of numerous investigations in the literature (e.g. Chang, 1970; Simpson, 1989). The boundary layer separation is a result of strong adverse pressure gradients in the direction of the flow and leads to increased energy losses. The general problem of turbulent boundary layer separation is sufficiently complex involving, for example, three-dimensionality, large-scale unsteadiness that most earlier studies in the literature have focussed attention on nominally two-dimensional separated flows (e.g. Stratford, 1959; Sandborn and Liu, 1968; Simpson et al., 1981; Viswanath and Brown, 1983; Simpson, 1985; Thompson and Whitelaw, 1985; Viswanath, 1988). While significant developments have taken place during the last decade in the calculation methods for separated flows, difficulty in modelling turbulent stresses in such flows still remains (Marvin, 1993). Carefully planned building-block experiments involving measurements of mean as well as turbulence quantities have been of great value in improving aspects of turbulence modelling for separated flows (Marvin, 1982, 1983; Simpson, 1987; Williams, 1989).

Separation control by passive or active means is widely employed for improving aerodynamic performance. The monograph by Chang (1976) contains an excellent account of several passive and active methods of separation control in different speed regimes. Recent reviews on the subject include that of Gad-El-Hak and Bushnell (1991) and Wygnanski (1997). Tangential blowing, which involves injection of fluid parallel to the wall through a narrow slot, is generally known to be an effective means of separation control (Peake, 1966; Viswanath, 1988; Wong, 1977); the injected mass energizes the boundary layer near the wall providing sufficient kinetic energy to negotiate adverse pressure gradients. Since blowing involves injection of additional mass and momentum into the boundary layer, the parameters affecting its performance include the jet velocity, density and the slot height (in two-dimensional flows). The most widely used and relevant parameter (Lachmann, 1961; Chang, 1976) is the blowing momentum coefficient, C_μ, defined by

$$C_\mu = m_j U_j / \rho_0 U_0^2 \theta_0$$

where m_j is the jet mass flow rate per unit span, U_j is the velocity, ρ_0 and U_0 are the (local) freestream density, velocity and θ_0 is the boundary layer momentum thickness.

just ahead of separation. Other definitions of C_μ have been employed as well in the literature (e.g. Chang, 1976) which utilize different velocity and length scales; for example, excess velocity $(U_j - U_0)$ is used instead of U_j for the momentum injected and a length scale of the body (e.g. airfoil chord in a 2D flow) is often used for normalization. Here we prefer a viscous scale like θ_0 since it would reflect a local boundary layer property; as a result, C_μ values so defined, will be generally an order of magnitude larger.

Among the several factors that may determine the effectiveness of injection, earlier studies (Peake, 1966; Viswanath, 1988) have shown that the injection slot location is a critical parameter. It is convenient to distinguish between two types of injection, depending upon the slot location:

(I) U-type: injection is upstream of separation point (i.e., the conventional location adopted for boundary layer control).

(II) D-type: injection is downstream of separation point, but within the recirculation zone.

Viswanath et al., (1983) discussed briefly some of the difficulties associated with U-type injection in the supersonic case and provided the first assessment of D-type injection effectiveness in a ramp-induced turbulent separated flow at a Mach number of 2.50; based on measurements of surface pressure distributions and limited pitot pressure survey in the interaction region, they showed that D-type injection was more effective than U-type. Beyond these early observations, there has been no attempt in the literature assessing either the general effectiveness of D-type injection to other separated flows or its exploitation in design applications.

It is to be recognized that studies involving tangential blowing or injection have been reported in other flow situations; for example, to provide lift enhancement on airfoils and wings using trailing-edge blowing which may involve D-type injection (Lachmann, 1961). In contrast, the emphasis and focus in the present work is on the suppression of boundary layer separation to reduce severity of viscous effects.

In this paper, we present new results from an experimental programme specifically designed to assess in detail the effectiveness of D-type injection in a low speed separated flow. Turbulent boundary layer separation occurred on an axisymmetric contoured afterbody due to sustained adverse pressure gradients. Based on surface pressure and detailed flow-field measurements employing a 2-compo-

nent LDV system, it is explicitly demonstrated that D-type tangential injection can be an effective means of separation control, considering both wall and wake flow reversals.

2
Experiments

2.1
Test facility and model configuration
The experiments were performed in the 0.91 m dia. low speed wind tunnel at a freestream velocity (U_∞) of 20 m/s. The axisymmetric model configuration employed had a diameter (D) of 122 mm and a total length of 1420 mm made up in 3 sections: a tangent ogive nose 300 mm long, a central cylindrical section 1047 mm long and a circular arc afterbody (of radius of curvature = 128 mm) 98 mm long (Fig. 1); the afterbody also carried a sting of 30 mm dia. and 330 mm long on which the separated flow reattached. Two afterbody models were fabricated for making measurements, both with and without flow control. Figure 1 shows the afterbody model with facility for tangential blowing with an annular axisymmetric slot height (h) 2.5 mm (Fig. 1): sufficient care was taken in the slot design to ensure tangential injection and the above value of h was chosen primarily from supersonic experience (Viswanath et al., 1983). The slot location $(x = -15$ mm) was chosen so that it is downstream of the separation point (in the absence of injection) but within the reversed flow zone based on preliminary experiments. The model was supported with a thin rectangular strut at a distance of 300 mm from the nose which also provided the passage for the jet flow into the model.

2.2
Instrumentation and measurements
Model static pressure distributions on the cylinder and afterbody were measured using Furness Control micromanometers primarily on the lee-ward (top) generator (limited measurements at a few other generators on the afterbody were carried out as well); these measurements were made at three values of blowing or injection velocity (U_j) of 15, 25 and 31 m/s; the jet mass flow was calculated using a rotometer installed in the jet flow circuit.

The flow measurements of the mean and turbulent quantities were made using a three-beam, two-component DANTEC laser Doppler velocimeter. The LDV was used in the forward scatter mode to achieve higher signal-to-noise ratio. The focal length of the front lens was 600 mm and
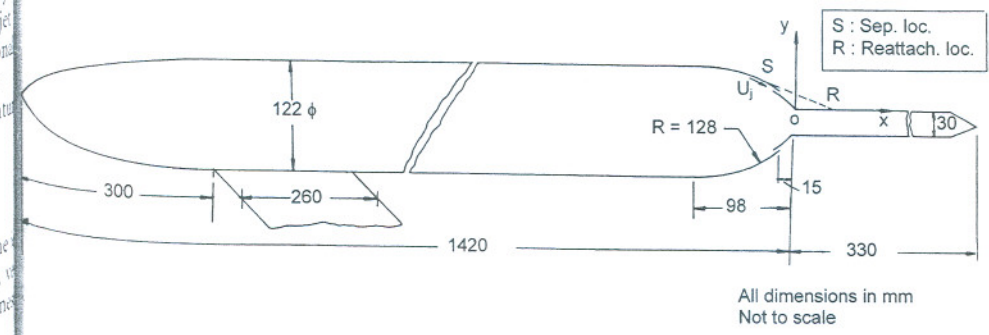
Fig. 1. Schematic of axisymmetric model

All dimensions in mm
Not to scale

the beam intersection angle was 4.66°. The ellipsoidal probe volume had a length of about 2 mm and a diameter of 0.2 mm. Fringe spacing in the blue and green components were 6.8 and 6.0 µm respectively. A Bragg cell with an optical frequency shift to 40 MHz was used for measuring the reversed flow; in addition, an electronic frequency shift was also used for accurate measurement of low velocities. Data from the counter-type signal processor was transferred to the PC/AT system using DMA-based high-speed digital I/O cards. All the software modules, including those for acquiring Doppler data from DIO of counter processor, LDV parameter selection, quick check of on-line data and processing of data were developed at NAL (Ramesh et al., 1994).

The mean velocity, turbulent shear stress and two-component turbulent kinetic energy measurements were made with optics in the ±45° configuration; limited mean velocity data and intermittency measurements, (characterising the fraction of time the flow is reversed) in the vicinity of separation location were carried out with optics in the 0/90° configuration.

Seeding was accomplished successfully using a smoke generator with liquid paraffin developed in our laboratory. It was found that paraffin smoke provided sufficiently good particle concentration even within the recirculating zones of the flow. No direct estimate of the particle sizes was made; however, we expect that the particle size is in the range of 2 to 5 microns, as reported by Wiedemann (1994). The data rates were typically in the range 400 to 600 samples/s. Data validation rates were in the range of 500 to 800 for a batch of 1000 samples, which is generally indicative of good SNR conditions.

In the present experiments involving measurements in a separated flow, preliminary studies were made to arrive at an optimum ensemble size for determining the statistics in the attached and reversed flow zones. Although 5000 samples were found adequate for obtaining good repeatability of mean velocities in the attached (or forward) flow regions, the quality of the turbulent shear stress and kinetic energy data showed visible improvements with 10,000 samples. So, a minimum ensemble size of 10,000 samples was adopted for obtaining the mean as well as the turbulent quantities in zones with $u > 0$. A similar exercise for the reversed flow region ($u < 0$) suggested that an ensemble size of 20,000 samples should be adequate which was finally adopted.

2.3
Estimates of uncertainty in the measured data

For the LDV data, sources of error include optical, statistical and positional. The uncertainty in the measurement of beam half-angle is estimated to be ±0.01° which translates to an uncertainty in velocity of ±0.05 m/s; however, the resolution of the burst counter results in a relatively higher uncertainty of ±0.1 m/s. For the sample size used for each data point (discussed above) we expect the statistical errors to be small (<1%). No correction for the measured data for possible velocity bias was made since such corrections did not seem warranted based on comparisons of measurements in certain standard flows as well as redundancy measurements (Ramesh et al., 1995);

such an observation has also been made by Admas and Eaton (1988) in low speed separated flow. Furthermore, reliable corrections schemes are not established for velocity bias. Likely errors in the measured mean velocity, turbulent shear stress and 2-component kinetic energy data are given below; these estimates are based on repeatability tests and comparison with redundancy measurements, wherever possible.

Quantity	Error
Pressure coefficient, C_p	≤±0.3%
Mean velocity, u	≤±2% or 0.1 m/s whichever is higher
Turbulent shear stress (τ)	≤±6%
Turbulent kinetic energy (k)	≤±8%
x	≤±0.5 mm
y	≤±0.3 mm

3
Results and discussion

3.1
Without tangential blowing

3.1.1
Boundary layer properties on the cylinder

The measured mean velocity profile on the cylinder at $x = -258$ mm showed features of a well developed turbulent boundary layer with the following properties (Ramesh et al., 1995):

Boundary layer thickness (δ) = 25 mm
Displacement thickness (δ^*) = 3 mm
Momentum thickness (θ) = 2.3 mm
Wall skin friction coefficient (C_f) = 0.0036

3.1.2
Surface pressure distributions

The measured surface C_p distributions on the afterbody and sting along the top generator are shown in Fig. 2 (the results with blowing will be discussed in Sect. 3.2); the measured C_p on two side generators (90° apart) showed good agreement with those measured on the top generator suggesting good axisymmetry (Ramesh et al., 1995). The static pressure over a large part of the cylinder is essentially constant (Ramesh et al., 1995), decreases gradually as the flow expands around the cylinder – afterbody junction due to the change in surface curvature and is followed by a strong adverse pressure gradient leading boundary layer separation as seen by the pressure plateau; this is followed by a reattachment pressure rise and a pressure decay to freestream value on the sting.

The streamwise development of velocity profiles (Fig. 3), covering all the way upstream of separation and downstream of reattachment, show features typical of adverse pressure gradient boundary layer flow eventually leading to separation; the separation (x_s) and reattachment locations (x_R) are identified at $x = -28$ mm (±1 mm)
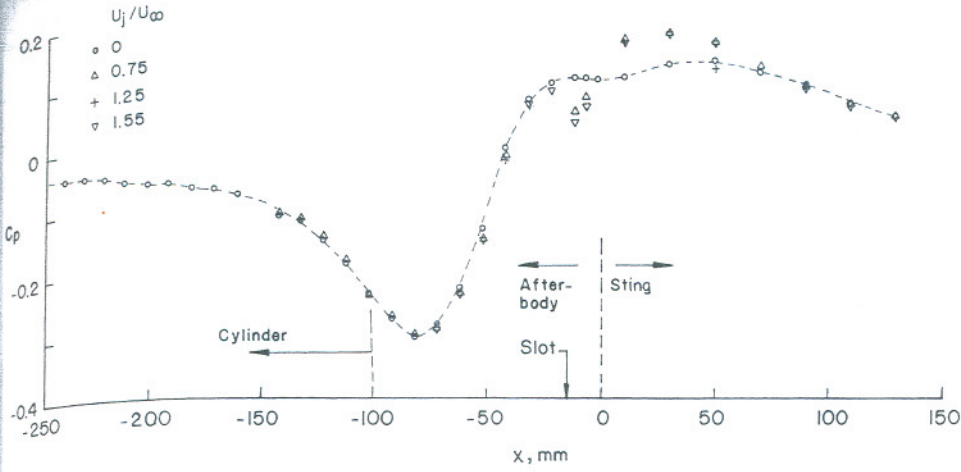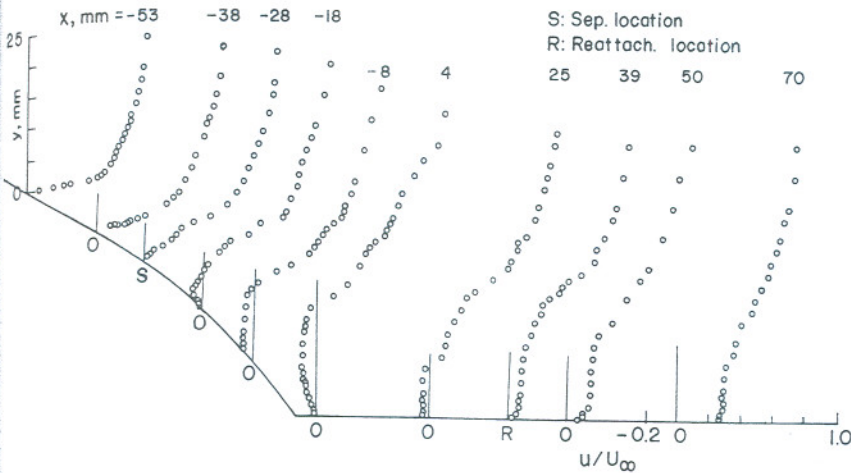
Fig. 2. Model static pressure distributions

Fig. 3. Mean velocity profiles in the separated zone

39 mm (±1 mm) respectively from the measured velocity profiles.

An important property related to unsteady aspects of separation is the wall flow intermittency (γ) which characterizes the fraction of the time the flow is reversed ($u < 0$) near the wall. Figure 4 shows that intermittent separation begins around $x = -38$ mm, which implies a distance of about $0.5\delta_0$ ahead of the time-averaged separation point (x_s); the value of γ is about 0.9 at x_s.
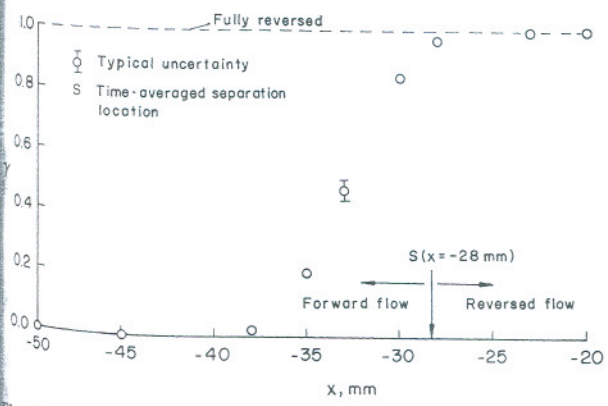

Fig. 4. Wall flow intermittency distribution

3.2
With tangential blowing

3.2.1
Surface pressure distributions
Results of surface pressure distributions on the afterbody and sting with tangential blowing are included in Fig. 2. The pressures on the cylinder and those on the afterbody ahead of separation ($x_s = -28$ mm) show little change due to blowing. However increased pressure gradients and increased static pressure recovery are evident at all three values of blowing velocity indicating favourable effects of injection. In particular, the pressure plateau region associated separation is completely eliminated with blowing, suggesting suppression of wall flow reversal even for a jet velocity ratio (U_j/U_∞) = 0.75. The dip in C_p values (immediately downstream of the slot) reflects the local static pressure of the jet associated with increasing value of U_j.

3.2.2
Mean velocity profiles
The mean velocity profiles (normalised by freestream velocity, U_∞) at four critical streamwise stations as affected by blowing are displayed in Fig. 5; as stated earlier, $x = -28$ and 39 mm correspond to the separation and reattachment locations without blowing. The elimination
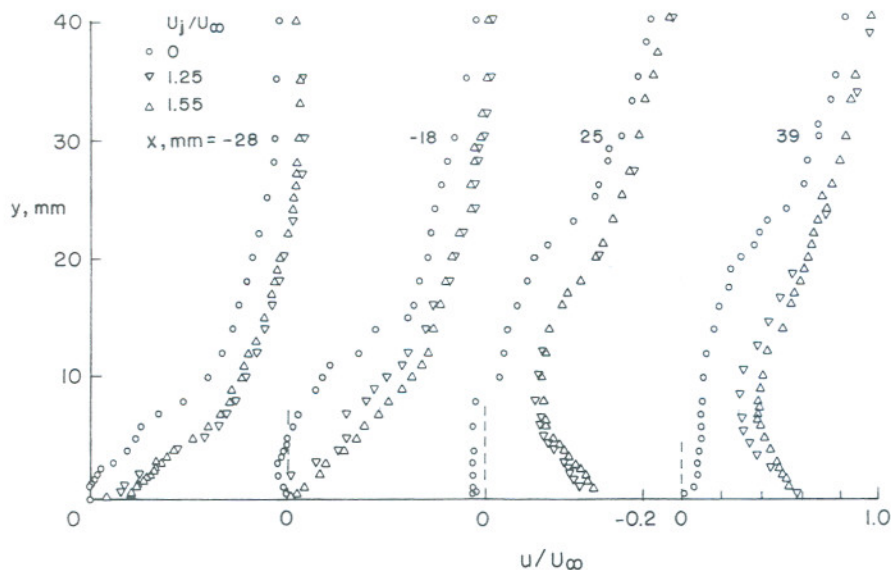
Fig. 5. Effect of blowing on mean velocity profiles

of the reversed flow in the separated zone ($x = -18$ mm, 25 mm: Fig. 5) at both values of U_j (=1.25 and $1.55U_\infty$) is consistent with the observed features of the surface pressure distributions discussed above. At all four stations, increased mean velocities all across the layer suggest efficient mixing of the injected jet with the surrounding flow. The jet mass flow at $U_j = 25$ and 31 m/s correspond to 13 and 16% (respectively) of the mass flow in the boundary layer at separation ($x_s = -28$ mm).

3.2.3
Boundary layer integral parameters
The streamwise variations of boundary layer displacement and momentum thickness distributions, corresponding to blowing at $U_j = 1.55U_\infty$ (and without it) are presented in Fig. 6; as may be expected, due to the elimination of the reversed flow as well as increased mean velocities, both δ^* and θ values are significantly lower with blowing.
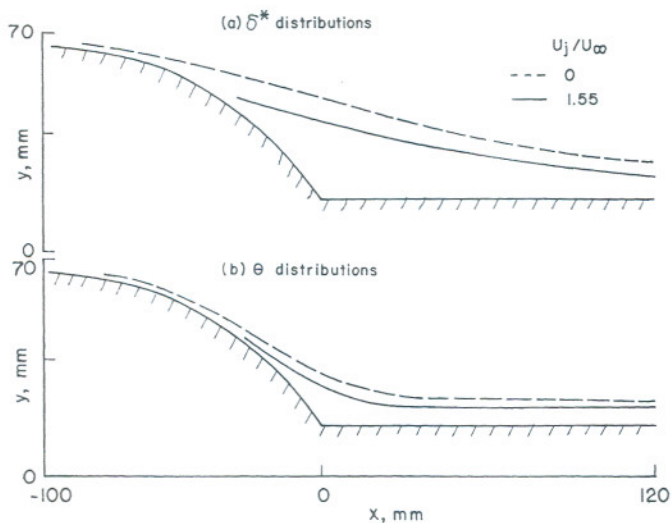

Fig. 6. Boundary layer displacement and momentum thickness distributions

3.2.4
Turbulent shear stress and kinetic energy profiles
The variations of the normalised turbulent shear stress and 2-component turbulent kinetic energy profiles at the highest jet velocity ratio of 1.55 are presented in Figs. 7 and 8 respectively. The complex qualitative nature of the shear stress profiles can be explained from the corresponding mean velocity profiles shown in Fig. 5. At $x = -28$ and -18 mm (i.e., ahead of the slot location), the downward shift of the location of τ_{max} is consistent with the increased mean velocities and velocity gradient near the wall due to blowing. At $x = 25$ and 39 mm, the shear stress profiles exhibit two peaks corresponding to the positive and negative maximum (normal) velocity gradients which can be observed in the mean velocity profile (Fig. 5); these profiles resemble 2D wake flow with a velocity minimum. A third peak in the shear stress which to be expected close to the wall in the (jet) wall boundary layer has not been captured in the measurements since occurs very lose to the wall ($y < 0.5$ mm); in fact, at $x = 39$ mm, measurement at the first y location from the wall reveals positive shear stress as expected.

The turbulent kinetic energy profiles at $x = -28$ and -18 mm show features qualitatively similar to the shear stress profiles (Fig. 7); in particular, the downward shift the y location corresponding to k_{max} may be seen. The increased k levels near the wall at $x = 25$ and 39 mm obviously arise form the increased (normal) velocity gradients and τ levels in the attached boundary layer with blowing. Detailed analysis of the mean flow and turbulent quantities with blowing from the point of view of turbulence modelling is currently in progress.

3.2.5
Blowing requirements
In the context of separation control, suppression of wall flow reversal may be adequate in certain applications (e.g relief in surface heat transfer at high speeds), while suppression of both wall and wake flow reversal may be important in other cases (e.g. aircraft intakes). Estimates blowing mass flow and momentum coefficient for the
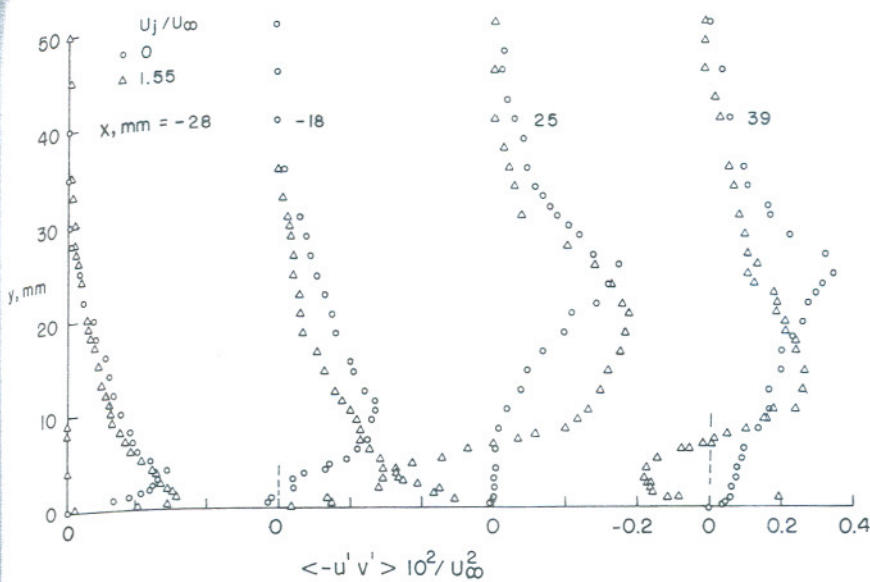
Fig. 7. Effect of blowing on Reynolds shear stress profiles

axisymmetric case ($C_{\mu A}$) are given in the Table below: $C_{\mu A}$ is defined as

$$C_{\mu A} = m_j U_j / \rho_0 U_0^2 \theta_0(D)$$

where m_j is the mass flow rate through the annular (axisymmetric) slot and D is the model forebody diameter (=122 mm). It is to be noted that the value of $C_{\mu A}$ quoted above is an order of magnitude higher (than what one would estimate using a body length scale) since we have used θ_0 as the relevant scale.

Blowing requirements

U_j/U_∞	$C_{\mu A}$	m_j/m_{bl}	Remarks
0.75	0.55	0.078	Suppression of wall flow reversal
1.25	1.55	0.130	Near suppression of wall and wake flow reversals
1.55	2.40	0.160	Complete suppression of wall and wake flow reversals

3.2.6
Possible flow mechanisms associated with D-type blowing

The effectiveness of D-type blowing has been demonstrated and it is informative to speculate on possible flow mechanisms associated with it. In this technique, it is the separated bubble which is energized by the tangential jet. The wall flow reversal is first suppressed by the interaction of the jet (having higher total pressure or longitudinal momentum) with the (otherwise) reversed-flow boundary layer. Second, the fluid injection causes a strong mass imbalance in the bubble and altered shear layer entrainment characteristics. Finally, the jet entrainment of the reversed flow in the bubble is possibly a strong factor promoting increased mixing leading to higher (mean) kinetic energy levels near the wall. These features result in the removal or elimination of the shear layer reattachment.

4
Conclusions

It has been demonstrated through detailed flow measurements for the first time that tangential blowing through a
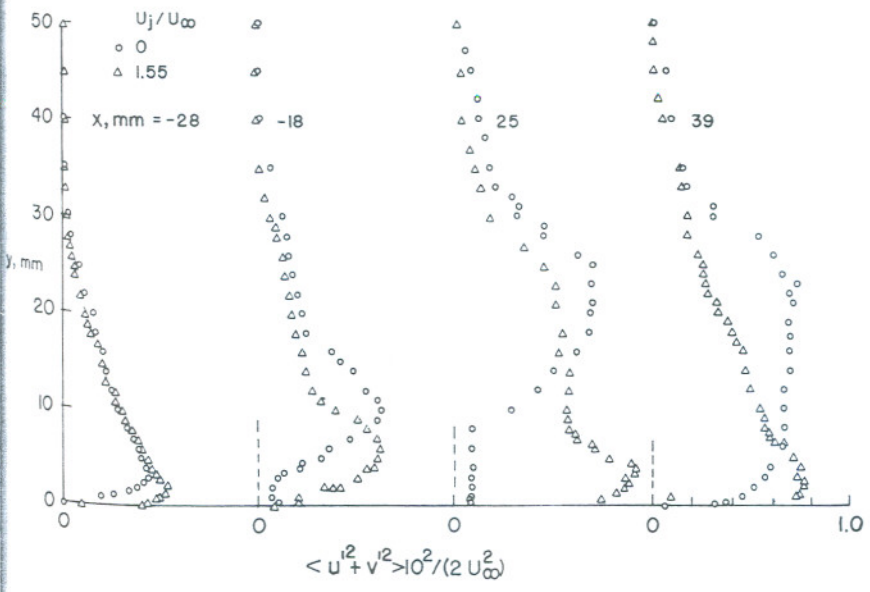

Fig. 8. Effect of blowing on turbulent kinetic energy profiles

narrow slot downstream of separation, but within the bubble, can be an effective means of separation control. D-type injection or blowing involves energizing the bubble flow leading to the elimination of shear layer reattachment, as opposed to energization of the boundary layer upstream of the separation point, which is the conventional technique adopted for boundary layer control. The mechanics of D-type blowing is therefore associated with manipulation of shear layer reattachment process which is a key element in the dynamics of separated flows as emphasized by Roshko (1966, 1967). Taken together with the success of D-type injection observed in a supersonic ramp flow (Viswanath et al., 1983), it may be concluded that D-type tangential blowing concept, although unconventional, may have significant potential for controlling separated flows in other situations (e.g. high-lift flows, shock-boundary layer interaction on supercritical airfoils). There is scope for optimizing the injection parameters for improved performance.

The experimental results presented in this paper also provide on excellent data base on an axisymmetric separated flow useful for improving turbulence modelling as well as CFD code validation.

References

Adams EW; Eaton JK (1988) An LDV study of the backward facing step flow, including the effects of velocity bias. J Fluids Eng 110: 275–282

Chang PK (1970) Separation of Flow, Pergamon Press

Chang PK (1976) Control of Flow Separation, Hemisphere Publishing Corporation

Gad-El-Hak; Bushnell DM (1991) Separation control: Review J Fluids Eng 113: 5–30

Lachmann GV Ed (1961) Boundary Layer and Flow Control, Vol. I, Pergamon Press

Marvin JG (1982) Turbulence modelling for computational aerodynamics, AIAA Paper 82-0164

Marvin JG (1983) Turbulent modelling of turbulent separated flows for aerodynamic applications, NASA TM 84392

Marvin JG (1995) Perspective on CFD validation, AIAA J 33: 1778–1787

Peake DJ (1966) The use of air injection of prevent separation of the turbulent boundary layer in supersonic flow. Aeronautical Research Council (UK) report CP 890

Ramesh G; Madhavan KT; Viswanath PR (1995) LDV measurements in an axisymmetric separated flow, Part I: Without flow control, National Aerospace Laboratories Report PD EA 9505

Ramesh G; Madhavan KT; Geetha E; Kusuma Suresh (1994) PC based data acquisition and processing software for two-component Doppler Velocimetry. Paper presented at the 19th National Symposium on Instrumentation, Tirupathi, India: 23–24

Roshko A (1966) A look at our present understanding of separated flows. Paper presented at the AGARD Symposium on Separated Flows, May 10–13, Brussels

Roshko A (1967) A review of concepts in separated flows. Paper presented at the Canadian Congress of Applied Mechanics, May 22–26, Quebec, Canada

Sandborn VA; Liu CY (1968) On turbulent boundary layer separation, J Fluid Mech 32: 293–304

Simpson RL; Chew YT; Shivprasad BG (1981) The structure of a separating turbulent boundary layer, Part I: Mean flow Reynolds stresses. J Fluid Mech 113: 23–51

Simpson RL (1985) Two-dimensional turbulent separated flow Agardograph 287

Simpson RL (1987) A review of two-dimensional separated flow calculation methods, In: Smith FT; Brown SN (eds). Proc IUTAM Symposium on Boundary Layer Separation 179–196

Simpson RL (1989) Turbulent boundary layer separation In: Lumley JL; Van Dyke M; Reed HL (eds) Ann Rev Fluid Mech Published by Annual Reviews Inc. USA, vol 21: 205–234

Stratford BS (1959) An experimental flow with zero skin friction throughout its region of pressure rise. J Fluid Mech 5: 17–35

Thompson BE; Whitelaw JH (1985) Characteristics of a trailing edge flow with turbulent boundary layer separation. J Fluid Mech 157: 305–326

Viswanath PR (1988) Shock wave-turbulent boundary layer interaction and its control: A survey of recent developments. Sadhana, Indian Academy Journal in Engineering Sciences 12: 45–104

Viswanath PR; Brown JL (1983) Separated trailing-edge flow. AIAA J 21: 801–809

Viswanath PR; Sankaran L; Sagdeo PM; Narasimha R; Prabhu (1983) Injection slot location for boundary-layer control in shock-induced separation. J Aircraft 20: 726–732

Weidemann J (1994) Laer Doppler Anemometrie, Springer Verlag Berlin

Williams BR (1989) Viscous-inviscid interaction schemes for separated flow, In: Proc. of Symposium on the Prediction and Exploitation of Separated Flow, Published by Royal Aeronautical Society, 5.1–5.16

Wong WF (1977) Application of boundary layer blowing to suppress strong shock-induced separation in supersonic inlet AIAA Paper 77–147

Wygnanski I (1997) Boundary layer and flow control by periodic addition of momentum. AIAA Paper 97-2117